Statistical Analysis of Reinforcement Characterization in SiC Particle Reinforced Al Matrix Composites

Peng Zhang and Fuguo Li†
School of Materials Science and Engineering, Northwestern Polytechnical University, Xi′an 710072, China
[Manuscript received July 15, 2008, in revised form October 9, 2008]

The characterization of reinforcement in 15% SiC particles reinforced Al matrix composites processed by powder metallurgy route was studied by statistical method. During the analysis, a new approach for the estimation of the characterization of reinforcement was presented. The mathematic software MATLAB was used to calculate the area and perimeter of reinforcement, in which the image processing technique was applied. Based on the calculation, the fractal dimension, shape factor, reinforcement size distribution and reinforcement distribution were investigated. The results show that the reinforcement shape is similar to rectangle; the reinforcement size distribution is broad with the range of 1–12 μm; the topography of reinforcement is smooth; and the reinforcement distribution is inhomogeneous. Furthermore, the cell model based on the statistical characterization was established and tested.

KEY WORDS: Particle reinforced Al matrix composites; Fractal dimension; Shape factor; Distribution; Cell model

1. Introduction

Metal matrix composites (MMCs) reinforced by particles are gradually popular due to their excellent properties such as high strength, high specific stiffness, high thermal and electrical conductivity, low density and flexible fabricating techniques. Because of these properties, MMCs have emerged as potential alternatives to conventional alloys in aerospace, automotive, recreation[1–4]. However, these properties are affected by many variables such as reinforcement size, morphology and distribution. Therefore, microstructure of composites plays an important role in determining the mechanical properties of these materials.

In the past decades, some experiment researches have found that the influence of reinforcement morphology on the mechanical properties of composites comes from the stress state[5,6]. In the location of sharp-angle of reinforcement, the stress is great because of the stress concentration. As a result, the matrix can often produce fracture[7,8]. However circular reinforcement can exhibit plastic strain gradient distribution in interface between matrix and reinforcement, which brings forth high strength and high plasticity. The reinforcement size can basically lead to the failure of materials[9,10]. For example, large reinforcement (>10 μm) often results in the reinforcement fracture, while the reinforcement (∼5 μm) can lead to the interface debonding. Another very important attribute in deformation processing is the distribution of reinforcement. By now, many efforts are concentrating on improving the uniformity of reinforcement distribution. As a rule, reinforcement clustering can be caused by insufficient mixing or slow solidification rates. Consequently, the constraints exerted by the high elastic modulus of reinforcement on the matrix alter the stress field in the vicinity of a cluster, giving rise locally to triaxial stresses much higher than the remote stress[11–13], which often causes the MMC to fail at unpredictable low stress levels.

In this paper, we conducted a systematic investigation of reinforcement characterization by a new approach, including reinforcement size, shape and distribution. Furthermore, based on the statistical analysis, the cell model was established, considering the approximate shape, size, distribution and orientation of reinforcement.

2. Experimental

The material examined was aluminum alloy-silicon carbide composites made by a powder metallurgy route. Aluminum powder was blended with 15% volume of silicon carbide powder to make the SiCp/Al composites. The matrix material was formed from powdered Al alloy, and the nominal chemical compositions can be seen in Table 1.

Table 1 Nominal chemical composition of aluminum alloys (wt pct)

Cu	Mg	Mn	Fe	Si	Zn	Ti	Al
4.1	0.64	0.54	0.37	0.34	0.1	0.019	Bal.

Figure 1(a) shows the microstructure of composite, where each pixel has a particular color described by the amount of red, green, and blue. In case each of these components has a range 0–255, this gives a total of 255^3=16777216 different possible colors in the image. If there is a similar color in some location, it is too difficult to choose object from the original image. From Fig. 1, it can be seen that the edge of some reinforcements in the image is not clear so that the skeleton is difficult to define. Therefore, for the better discerning in some detail the microstructural features, it is necessary to apply special image processing techniques[14] such as threshold, background removal, opening, closing, dilation and erosion, to render the resulting image more suitable for the job to follow. Figure 1(b) expresses the binary image after image processing. In binary image, each pixel is just black or white. Since there are only two possible values for

† Corresponding author. Prof.; Tel.: +86 29 83070387;
E-mail address: fuguolx@nwpu.edu.cn (F.G. Li).

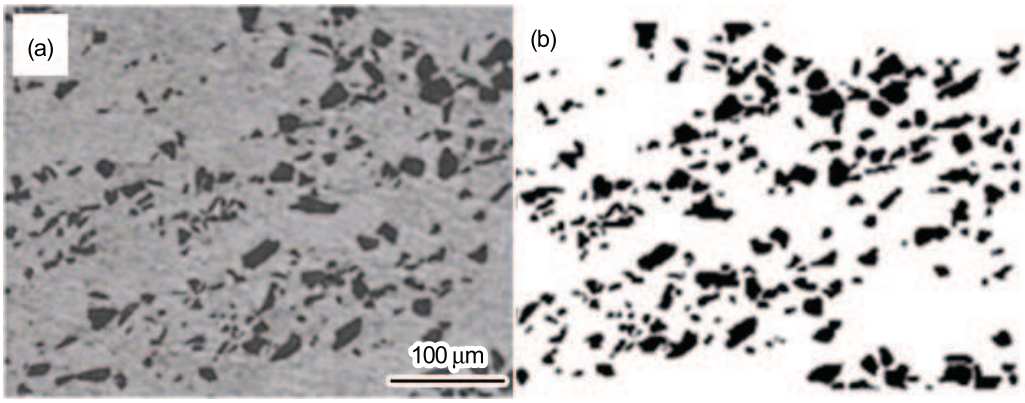

Fig. 1 Microstructure of a composite: (a) original image, (b) binary image

each pixel, some object in the image can be efficient to be obtained in terms of value of pixel.

3. Description of Reinforcement Characterization

The characterization of reinforcement was carried out by four basic descriptors commonly used in binary image, including shape factor, fractal dimension, size distribution and clustering distribution.

3.1 Shape factor

The effect of reinforcement on the composite is complex. Up to now, many studies of the effect of reinforcement on the deformation of composite have been undertaken by means of simulation. However, the shape of reinforcement embedded in the cell model is often supposed to be roundness, square, ellipse or rectangle without any reason[15–17], which is possibly improper. Therefore, the statistical description about shape is essential for further analysis. Here, for the analysis of the shape of reinforcement, the shape factor is adopted, given by

$$\text{shape factor} = \Phi^2/4\pi\mathrm{A} \tag{1}$$

where Φ is perimeter of reinforcement, A is area of reinforcement. The relation between shape factor and reinforcement shape can be seen in Table 2. It is clearly observed that the shape factor can show the aspect ratio of reinforcement. The smaller the shape factor, the smaller aspect ratio of reinforcement. On the contrary, the aspect ratio of reinforcement is great.

Table 2 Relation between shape factor and reinforcement shape

Reinforcement shape	Shape factor
Roundness	1.000
Square	1.273
Ellipse (1:2)	1.190
Ellipse (1:3)	1.518
Ellipse (1:4)	1.891
Rectangle (1:2)	1.432
Rectangle (1:3)	1.697
Rectangle (1:5)	2.292

3.2 Fractal dimension

In order to quantitatively evaluate the relationship between the minute roughness and reinforcements, the reinforcement outline was analyzed by using fractal dimension. The fractal dimension can be estimated through box-counting method or slit island method. Here, the slit island method was applied, which can be written in the following form[18]:

$$\ln \Phi = C + (D/2)\ln A \tag{2}$$

where Φ is the perimeter of particle, A the area of particle, and D the fractal dimension, which can be obtained from the slope of the plot of ln(perimeter) *vs* ln(area).

3.3 Reinforcement size

During the study, for the analysis of the size of reinforcement, the reinforcement size was characterized by the equivalent diameter d:

$$d = 4A/\Phi \tag{3}$$

where A is the area of reinforcement, and Φ is the perimeter of reinforcement.

From Eqs. (1)–(3), it is obvious that the area and perimeter of reinforcement play an important role in analysis. In this paper, for accurate calculating the area and perimeter of reinforcement, the concept of pixel was used. As a result, the description of area for reinforcement is defined as the total number of pixels of reinforcement, while the description of perimeter is defined as the total number of pixels of outline. Therefore, the precision is decided by the description of reinforcement shape. In the mathematic software MATLAB 6.5, the isolated reinforcement in the binary image can be captured, and furthermore, the skeleton can also be presented, as shown in Fig. 2. In general, the binary image is described by a matrix composed of 1 and 0. 1 means the foreground, and 0 means the background. Therefore, the value of area and perimeter are the total numbers of foreground pixels.

3.4 Clustering distribution

In reinforced MMCs, the clusters are zones where reinforcement cracking is the less dominant fracture mode than that in the other region. Generally, clustering can be quantified by measuring the near neighbor distance between the reinforcements; consequently, the narrower the distance, the more numer-

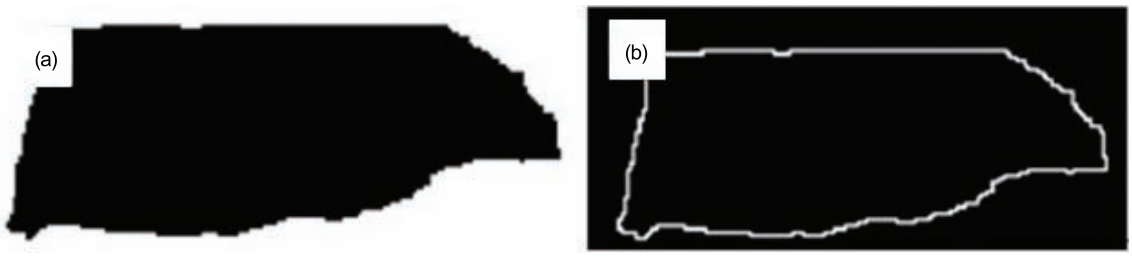

Fig. 2 Calculation for area and perimeter in binary image: (a) used for area calculation, (b) used for perimeter calculation

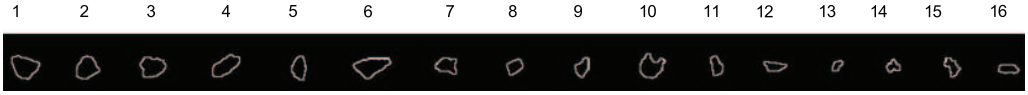

Fig. 3 Samples of reinforcements

ous the clusters. Here, the dilation in the software MALAB was applied to estimate the distribution of reinforcements.

Suppose that A and B are sets of pixels in a binary image. Then the dilation of A by B, denoted , is defined as

$$A \oplus B = \bigcup_{X \epsilon B} A_x \tag{4}$$

This means that for every point $x \epsilon B$, A is translated by those coordinates. In other words, dilation has an effect of increasing the size of an object. In MATLAB, when the dilation size of reinforcement is equal to the distance of neighbor, the reinforcement will grow so that it reaches the nearest reinforcement, and then they will form one unique object instead of two. As a result, the number of isolated reinforcements in the binary image decreases after dilation. This can be indicative of the characteristic distances of reinforcements. Figure 1 is at ×200 magnification, which is 510 μm×320 μm, including 834×522 pixels, each pixel corresponding to size of 0.61 μm.

4. Results and Discussion

4.1 Shape factor

The isolated reinforcements in Fig. 1 firstly were tagged with the serial number. In order to choose randomly the reinforcements from Fig. 1, the pseudo random numbers generator was used, which can be written as

$$X_{n+1} = CX_n(\text{Mod})M \tag{5}$$

where $CX_n(\text{Mod})M)$ means the arithmetical complement of dividing CX_n by M, while the value of parameters C, M, X_0 can be expressed as follows:

$$C = 5^{2p+1} \quad M = 2^q \quad X_0 = 1 \quad \text{or} \quad X_0 = 4m + 1$$

where the parameters p, q, m are positive whole numbers. During the calculation, suppose C=5 (p=0), M=64 (q=6), X_0=1, and in terms of Eq. (5), 16 pseudo random numbers can be obtained: 1, 5, 25, 61, 49, 53, 9, 45, 33, 37, 57, 29, 17, 21, 41, and 13. Based on these numbers, 16 reinforcements were obtained, as shown in Fig. 3. According to Eq. (1), the shape factor of these reinforcements was exhibited in Table 3.

Table 3 Shape factor of reinforcements

Serial number	Shape factor
1	1.130
2	1.048
3	1.143
4	1.215
5	1.164
6	1.419
7	1.353
8	1.117
9	1.220
10	1.500
11	1.247
12	1.595
13	1.204
14	1.435
15	1.958
16	1.554

From Table 3, it can be seen that the shape factor of reinforcements distributes in a range of 1.0–2.0. Within the range between 1.0 and 1.3, the number of reinforcements is 9; within the range between 1.3 and 1.5, the number is 4, while the rest lies within the range of 1.5–2.0. In addition, the mean value of shape factor for these reinforcements is 1.331. In contrast to Table 2, it can be found that the mean value exists between the square (1:1) and rectangle (1:2). Therefore, the shape of these reinforcements can be regarded as a rectangle (<1:2) for considering.

4.2 Fractal dimension

During the analysis of fractal dimension, 16 reinforcements discussed above were still used. The reinforcement of serial number 1 was given as an example to show the operation procedure. Firstly the area and perimeter of original reinforcement were calculated. Secondly, all the pixels in the image are ensured to produce an image with the same size as the original, only the reinforcement was carried out again at a suitable magnification at which the probability of finding any of the microstructural features was essential.

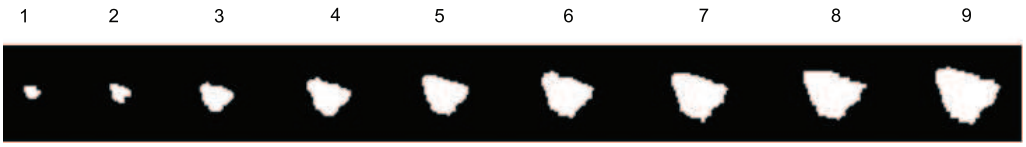

Fig. 4 Reinforcement magnified

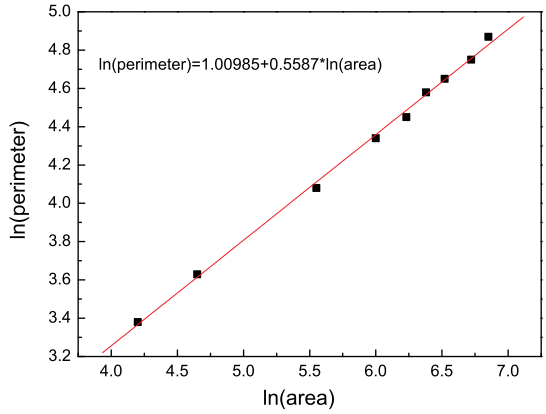

Fig. 5 Relation between ln(perimeter) *vs* ln(area)

Then the rest operation may be deduced by analogy, as shown in Fig. 4. As a result, the serial of area and perimeter of magnified reinforcement can be obtained, as listed in Table 4. According to Eq. (2), the fitting curve of ln(perimeter) *vs* ln(area) is plotted, as shown in Fig. 5. The fractal dimension of the reinforcement is the twice of slope, namely 1.117.

Table 4 Area and perimeter of reinforcement sample

Number	Area /pixel	Perimeter/pixel
1	66.875	29.000
2	104.375	37.350
3	263.000	60.125
4	414.875	76.750
5	497.000	84.875
6	602.875	99.750
7	700.875	107.500
8	795.625	115.000
9	930.875	130.375

Based on the method discussed above, the fractal dimension of rest reinforcements can also be obtained, as shown in Table 5. Apparently the fractal dimension of these reinforcements captured exists in the narrow range of 1.10–1.22. That is to say, the roughness of reinforcements is very similar to each other. In comparison with the fractal dimension of roundness, whose value is 1, the outline of these reinforcements, clearly as seen, are still smooth.

4.3 Size distribution

Quantitative analysis of reinforcement size distribution holds great importance in correlating the microstructural features of MMCs to their mechanic response. For the better predict of the reinforcement size distribution, it is vital that the quantity of reinforcements obtained must be as much as possible. For this reason, the method of random line incision was employed in the original image (Fig. 1). Accordingly the reinforcements incised were captured. Then the area and perimeter of these reinforcements obtained could be measured to calculate the equivalent diameter in terms of Eq. (3). And then the results calculated here were multiplied by 0.61 to get the actual value.

Table 5 Fractal dimension of reinforcement selected

Serial number	Fractal dimension
1	1.1174
2	1.16266
3	1.17186
4	1.18314
5	1.16972
6	1.14106
7	1.20768
8	1.18744
9	1.17782
10	1.16342
11	1.16235
12	1.17221
13	1.17361
14	1.17862
15	1.21058
16	1.16752

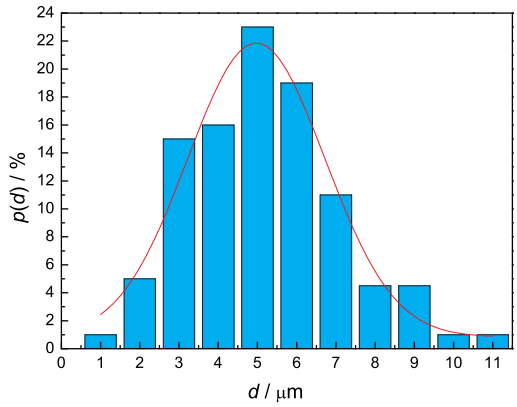

Fig. 6 Size distribution of reinforcements

By means of selection, 142 reinforcements can be obtained. The size distribution of these reinforcements is shown in Fig. 6. By fitting the size distribution, the equation can be expressed by the GaussAmp function, which is written as

$$p(d)=0.84213+21.02676\cdot\exp\left(-0.5\times\left(\frac{d-5.47086}{1.74902}\right)^2\right) \quad (6)$$

From Fig. 6, it is evident that the size distributes in the range of 1–12 μm, however the major lies within

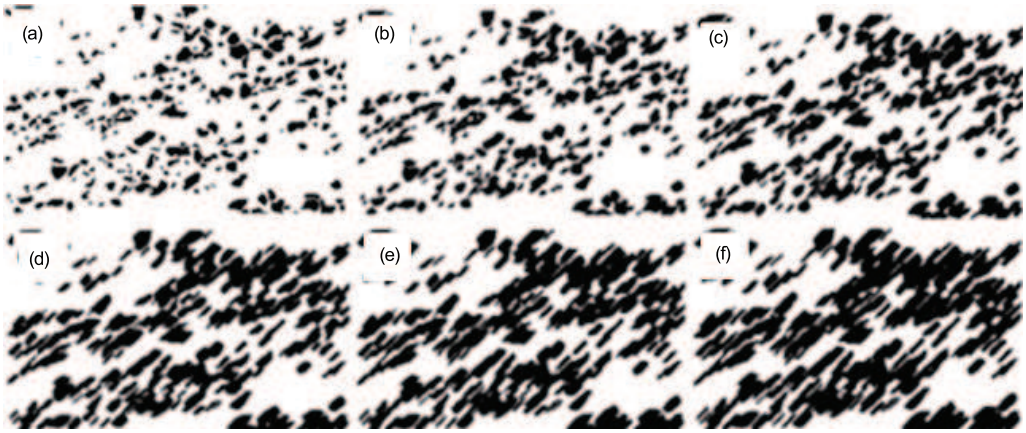

Fig. 7 Dilation procedure along 45°: (a) original, (b) 1st, (c) 2nd, (d) 3rd, (e) 4th, (f) 5th

3–8 μm. Studies on the fracture mechanism of metal matrix composite indicate that the reinforcement size dominates the rupture of MMC. For example, the large reinforcements (d>20 μm) are inclined to produce reinforcement fracture, while the interfacial debonding is often found around the small reinforcements (d<10 μm). Thus, from Fig. 6, we know that the fracture of the composites examined mainly results from the interfacial debonding.

4.4 Cluster

The estimation of cluster needs to count the quantity of isolated reinforcements. Figure 1 represents 256 isolated reinforcements. During the process of dilation, the operation is done in four directions: 0, 45°, 90°, and 135°. Each direction is operated for five times, and the dilation size is 3 pixels every time, namely 1.83 μm. Figure 7 shows the dilation process along 45°.

From Fig. 7, it is patently obvious that in the 3st dilation, the process reaches a characteristic inter-reinforcements distance, especially in the top right corner and down right corner of the image. Moreover there is a decrease in the number of isolated reinforcements, as shown in Table 6. The results suggest that along direction 45° and 135°, the cluster is more evident than the direction 0° and 90°. Three dilations represent a distance of 5.49 μm, which shows that only less than 100 isolated reinforcements exist in four directions as shown in Table 6. Therefore, the reinforcement distribution in the image takes on the obvious local cluster characters. It is well known to all the microstructural heterogeneities of composites give rise to the flow localization in the material during the deformation, which may lead to crack initiation, and ultimately failure. Consequently it is an imperative for the secondary processing of composites to achieve more uniform distribution.

5. Cell Model Based on the Statistical Characterization

5.1 Cell model

It is well known that the macroscopic mechanical behavior of MMCs depends on their microstructures.

Table 6 Quantity of isolated reinforcements after dilation

	0°	45°	90°	135°
1 (>3.66 μm)	179	155	175	162
2 (>7.32 μm)	124	102	126	97
3 (>10.98 μm)	81	63	83	59
4 (>14.64 μm)	58	45	61	42
5 (>18.3 μm)	41	32	44	34

Extensive investigations such as numerical analysis have been devoted to the effects of volume fraction and distribution of the second phase on the MMCs, where the unit cell model was usually applied[15,16,19]. In addition, the shape of the reinforcement was assumed to be cylindrical, spherical, rectangular or cubical. This simplification aids in computations but fails to capture the morphology such as size, spatial distribution, shape associated with metal matrix composite. In this paper, according to the statistical characterization of reinforcements, the cell model for metal matrix composite was established.

According to the shape factor of reinforcement, it is found that the shape of reinforcement can be taken as rectangle (<1:2), here the parameter 1:1.5 is captured; the reinforcement major size distributes in the range of 3–8 μm, here the equivalent diameter of 6 μm is used. Based on these data, in terms of Eq. (3), the long and short side of rectangle can be calculated, which are 7.5 and 5 μm.

One of the important parameters in cell model is volume fraction. In the unit cell, the model is often established as axisymmetry, where the matrix is embedded with regular shape reinforcement. Therefore, the model can be easily established according to volume fraction. However, based on the statistical characterization, multi-reinforcements cell model is difficult to be established according to the volume fraction. In this case, the new approach of area fraction was adopted, which is equal to the percent of dividing the foreground pixels by the whole pixels in the image, as shown in Fig. 1. Consequently, the result is 19.09%; meanwhile 285 reinforcements can be acquired. From Fig. 7, it is clear that the distribution of reinforcements can be divided into four zones, as depicted in Fig. 8(a). The area fraction of these zones were calculated respectively: zone I was accounted for 1.91%, zone II 8.44%, zone III 7.03%, and zone IV

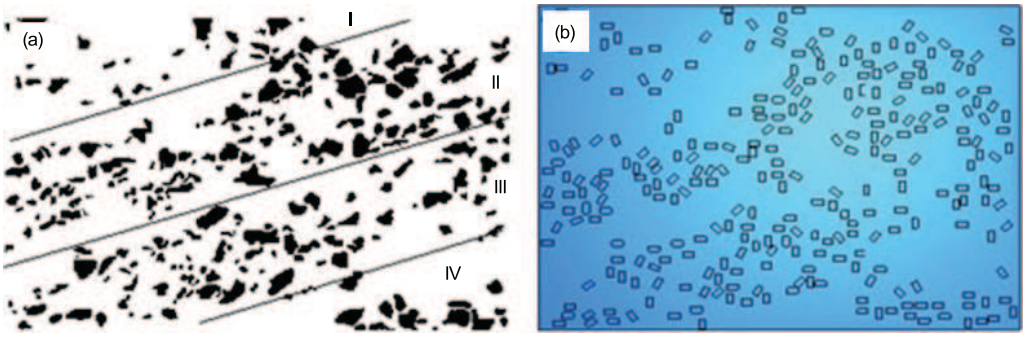

Fig. 8 Statistical model: (a) morphology of reinforcements, (b) cell model based on the statistical characterization

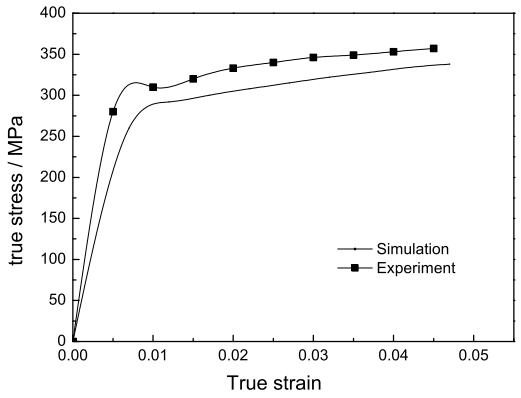

Fig. 9 Stress-strain curves of experiment and simulation

1.71%. Thus the quantity of four zones holds: 29 for zone I, 126 for zone II, 105 for zone III, 25 for zone IV. Finally according to the distribution of reinforcements in the original image, the cell model based on the statistical characterization is established, as shown in Fig. 8(b). Compared with the Fig. 8(a), the distribution of reinforcements in Fig. 8(b) shows the similarity.

5.2 Test of cell model

In order to validate the cell model, the finite element method was used. The cell model was imported into the software ABAQUS. The particle of SiC is assumed to be linear elastic, where the parameters Yong′s modulus is $E_{\rm p}$=440 GPa and Poisson′s ratio $v_{\rm p}$=0.17. The flow stress-strain relation of matrix Al is defined as $\sigma_{\rm Y}=\sigma_{\rm Y}^0+h(\bar{\varepsilon_{\rm p}})^n$, where $\sigma_{\rm Y}$ denotes flow stress, $\sigma_{\rm Y}^0$ the initial flow stress, h the hardening coefficient, $\bar{\varepsilon}_{\rm p}$ the equivalent strain, and n the hardening exponent. During the calculation, $\sigma_{\rm Y}^0$=250 MPa, n=0.455, h=173 MPa were used. The boundary condition is defined as U_y=0 at the bottom border, and the displacement load U_y is applied to the upper border to make the model 5% of deformation. Furthermore, to control the harmony of deformation, the order of equation in the software ABAQUS 6.3 was applied to keep the left and right border of model from distortion.

Figure 9 represents the stress-strain curves of experiment and simulation. It is obvious that the simulated result is lower than the experimented ones during the deformation. The possible reason is that the simulation model is based on the statistical analysis, in which the reinforcement size is assumed to be consistent, and materials failure is not taken into account. Consequently, the simulated result deviates from the experimented ones. However, the deviation of results lies within the range of 10%, and therefore, the model based on the statistical analysis is reliable.

6. Conclusions

A novel approach to study statistical characterizations of reinforcements for MMCs was put forward based on the binary image in mathematic software MATLAB. In the study, four characters were analyzed, including shape factor, fractal dimension, size and distribution. Finally, the cell model based on the statistical analysis was established. The basic conclusions that can be drawn from the studies are below.

(1) By means of the technique of image processed, the characterization of reinforcement was picked up.

(2) The average value of shape factor of reinforcements lies between the square (1:1) and rectangle (1:2); the fractal dimension locates in the range of 1.1–1.22, which shows that the outline of reinforcements is smooth; the size distributes within the range of 1–12 μm, but the major is in 3–8 μm; the distribution expresses that in some local place the cluster emerges.

(3) Based on the statistical characterizations of reinforcements, the cell model was established. Through test, it is found that the cell model is reliable.

REFERENCES

[1] G.Q. Tong and K.C. Chan: *Mater. Lett.,* 1999, **38**(5), 326.
[2] K.S. See and T.A. Dean: *J. Mater. Process. Technol.,* 1997, **69**(1-3), 58.
[3] A. Onat, H. Akbulut and F. Yilmaz: *J. Alloy. Compd.,* 2007, **436**(1-2), 375.
[4] X. Deng, N. Chawla and K.K. Chawla: *Acta Mater.,* 2004, **52**(14), 4291.
[5] A. Rabiei, L.Vendra and T. Kishi: *Compos. Pt. A-Appl. Sci. Manuf.,* 2008, **39**(2), 294.
[6] A. Miserez, R. Muller, A. Rossoll, L. Weber and A. Mortensen: *Mater. Sci. Eng. A,* 2004, **387–389**, 822.
[7] P. Lipetzky, S. Schmauder and H. Fischmeister: *Com-*

put. Mater. Sci., 1993, **1**(3), 325.
[8] S. Honle and S. Schmauder: *Comput. Mater. Sci.,* 1998, **13**(1-3), 56.
[9] M. Song, B.Y. Huang: *Mater. Sci. Eng. A,* 2008, **488**(1-2), 601.
[10] E. Ergun, K. Aslantas and S. Tasgetiren: *Mech. Res. Commun.,* 2008, **35**(4), 209.
[11] J. Segurado, C. Gonzalez and J. LLorca: *Acta Mater.,* 2003, **51**(8), 2355.
[12] K. Aldas and M.D. Mat: *J. Mater. Process. Technol.,* 2005, **160**(3), 289.
[13] J. Boselli, P.J. Gregson and I. Sinclair: *Mater. Sci. Eng. A,* 2004, **379**(1-2), 72.
[14] M. Li, S. Ghosh and O. Richmond: *Acta Mater.,* 1999, **47**(12), 3515.
[15] G.Z. Kang, X.J. Shao, S.J. Guo: *Mater. Sci. Eng. A,* 2008, **487**(1-2), 431.
[16] I. Tirtom, M. Guden and H. Yıldız: *Comput. Mater. Sci.,* 2008, **42**(4), 570.
[17] N. Srikanth and M. Gupta: *J. Alloy. Compd.,* 2005, **394**(1-2), 226.
[18] Y.P. Duan, P. Li, K.M. Xue, Q. Zhang and X.X. Wang: *Trans. Nonferrous Met. Soc. China,* 2007, **17**(6), 1199.
[19] S.B. Prabu, L. Karunamoorthy and G.S. Kandasami: *J. Mater. Process. Technol.,* 2004, **153-154**, 992.